

Supporting Information

White light emission properties of defect engineered Metal Organic Frameworks by encapsulation of Eu³⁺ and Tb³⁺

Himanshu Sekhar Jena^{†‡}, Anna M. Kaczmarek^{†‡#}, Chidharth Krishnaraj[†], Xiao Feng[†], Kanika Vijayvergia[†], Hilal Yildirim[†], Shu-Na Zhao[†], Rik Van Deun[‡], Pascal Van Der Voort^{†*}*

[†]COMOC, Center for Ordered Materials, Organometallics and Catalysis, Department of Chemistry, Ghent University, 9000 – Gent, Belgium

[‡]L3 – Luminescent Lanthanide Lab, Department of Chemistry, Ghent University, Krijgslaan 281-S3, 9000 Ghent, Belgium

Corresponding Authors

^{*}(P.V.D.V.) E-mail: Pascal.VanDerVoort@UGent.be

^{*}(H.S.J.) E-mail: Himanshu.jena@ugent.be

hsjena@gmail.com

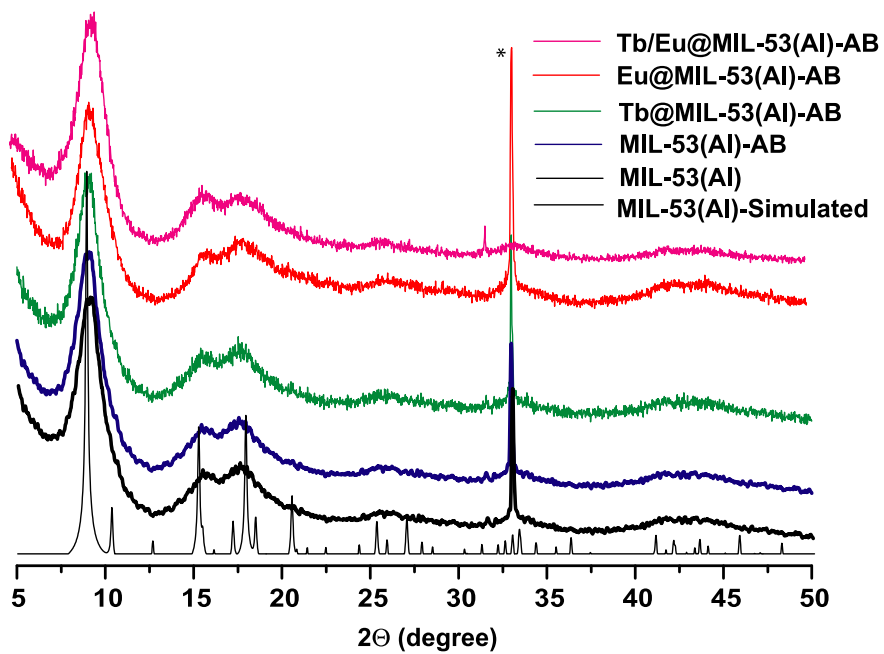


Figure S1. PXRD patterns of lanthanide encapsulated MIL-53(Al)-AB and Ln@MIL-53(Al)-AB (* peak from silicon sample holder).

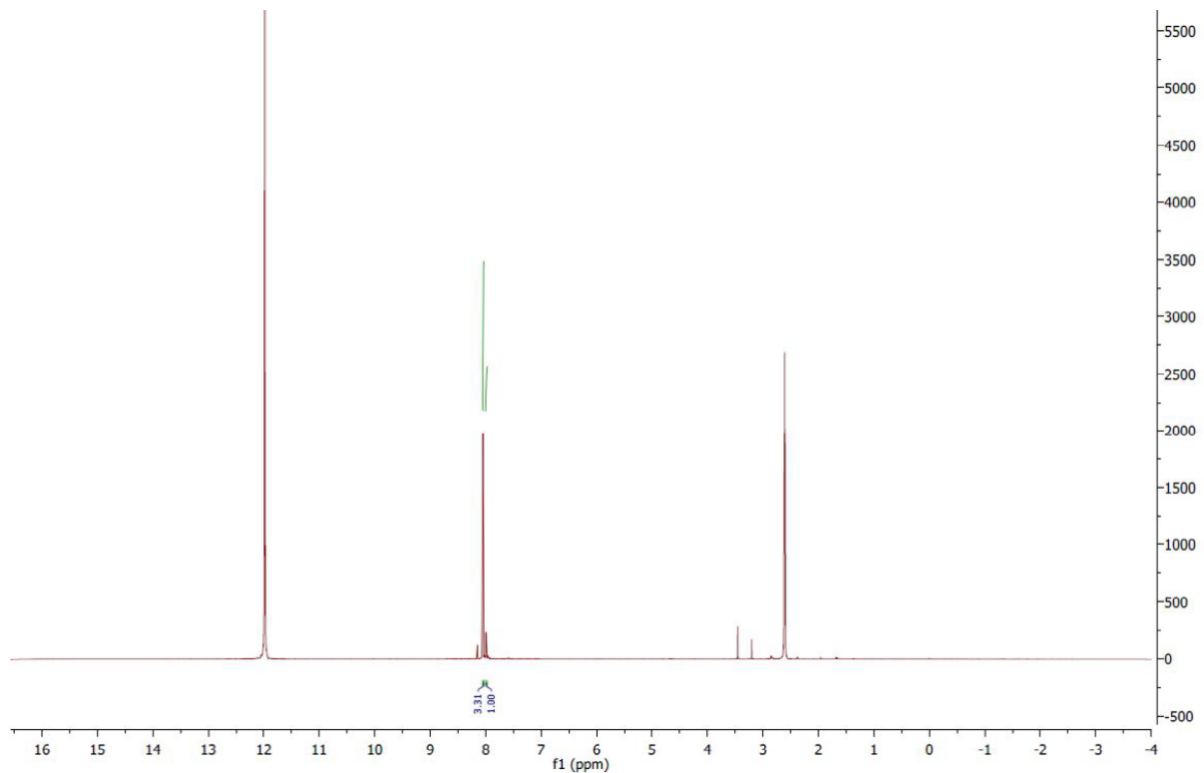


Figure S2. ^1H NMR of digested sample of UiO-66-AB in DMSO-d₆ (0.5mL) and D₂SO₄ (0.05mL)

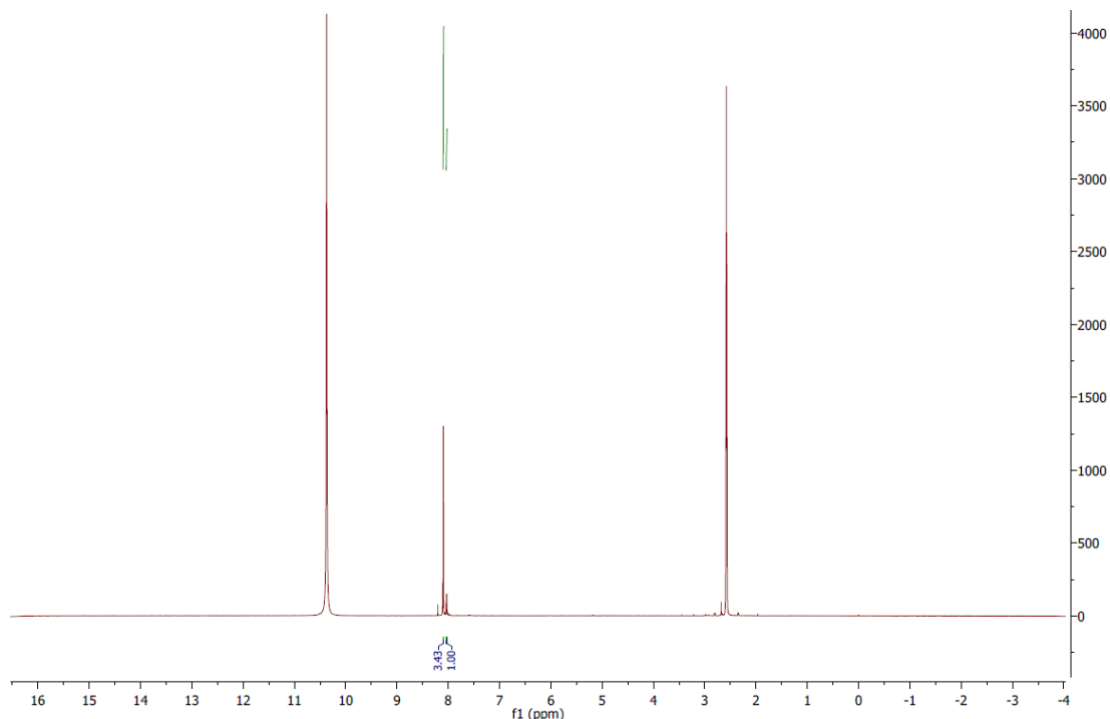


Figure S3. ¹H NMR of digested sample of MIL-53(Al)-AB in DMSO-d₆ (0.5mL) and D₂SO₄ (0.05mL).

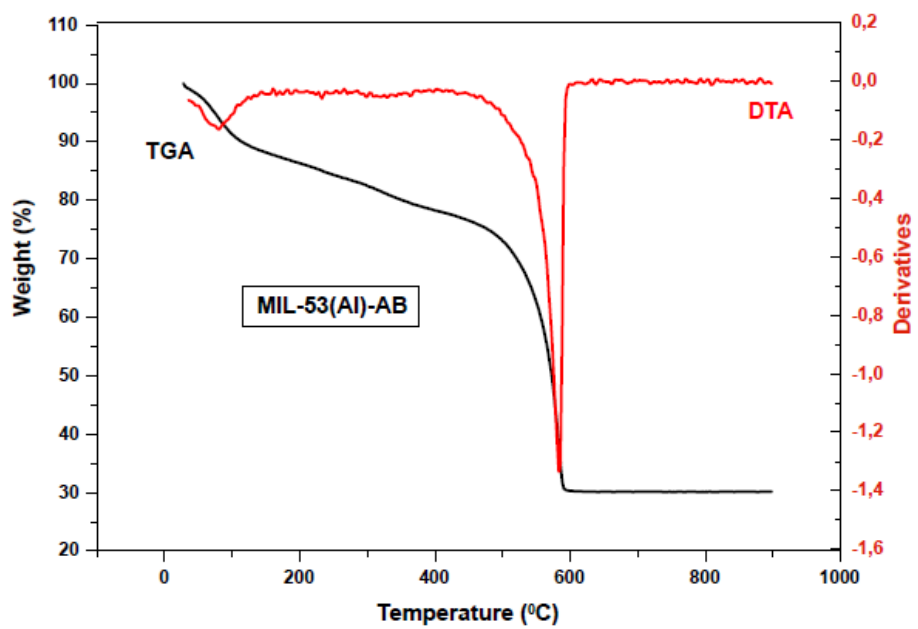


Figure S4. TGA spectrum of MIL-53(Al)-AB measured under air.

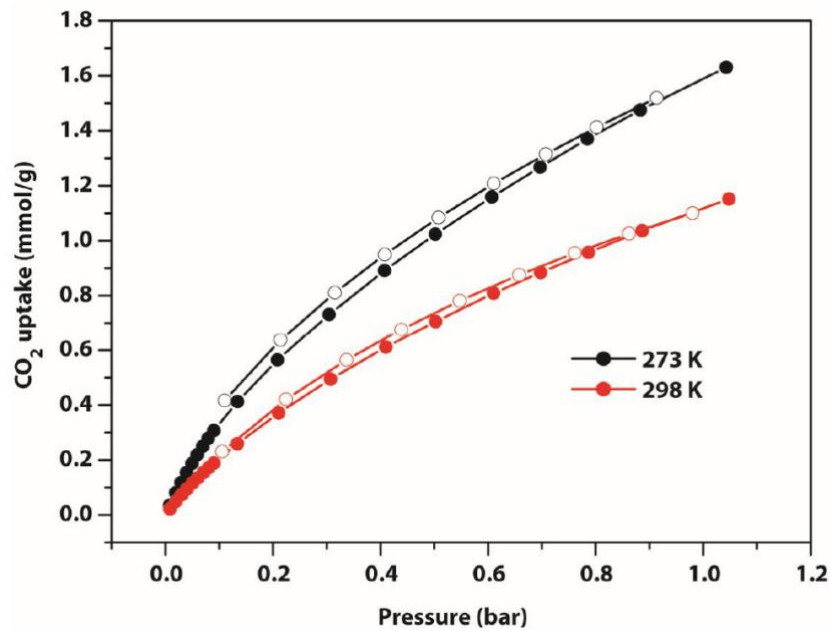


Figure S5. CO₂ adsorption/desorption isotherm of UiO-66-AB at two different temperatures.

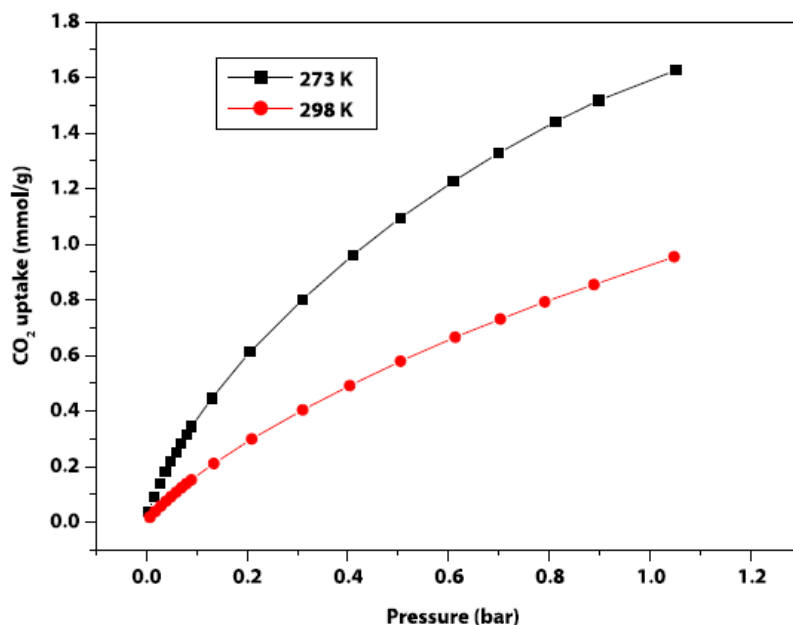


Figure S6. CO₂ adsorption isotherm of MIL-53(Al)-AB at two different temperatures.

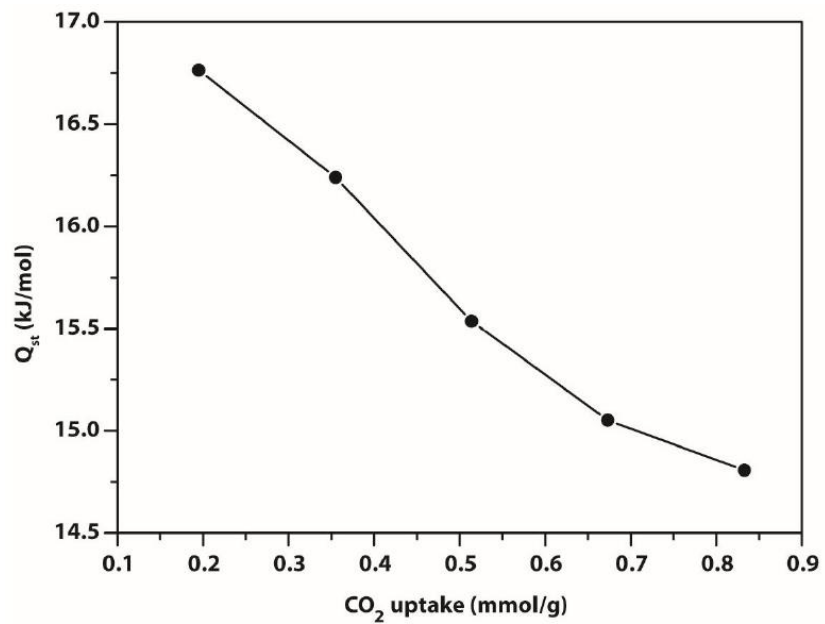


Figure S7. CO_2 isosteric heat of adsorption (Q_{st}) in UiO-66-AB using Clausius-Clapeyron equation.

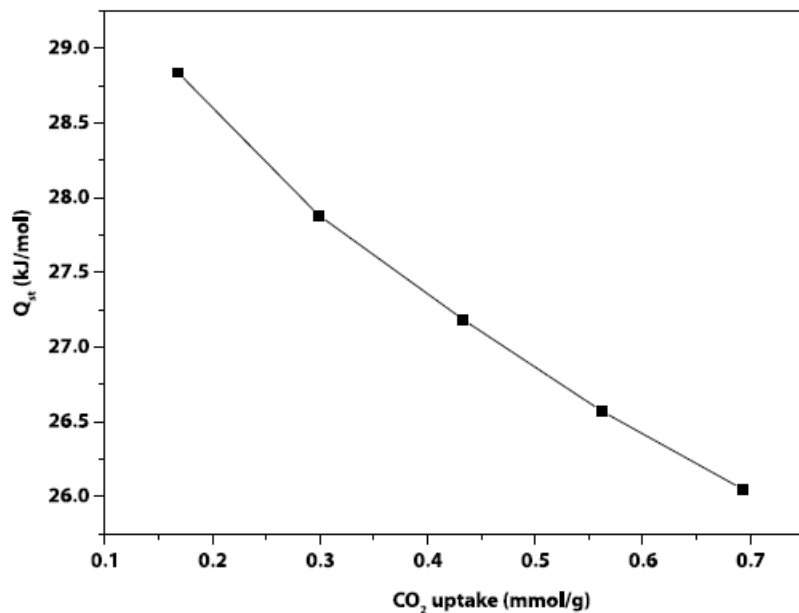


Figure S8. CO_2 isosteric heat of adsorption (Q_{st}) in MIL-53(Al)-AB using Clausius-Clapeyron equation.

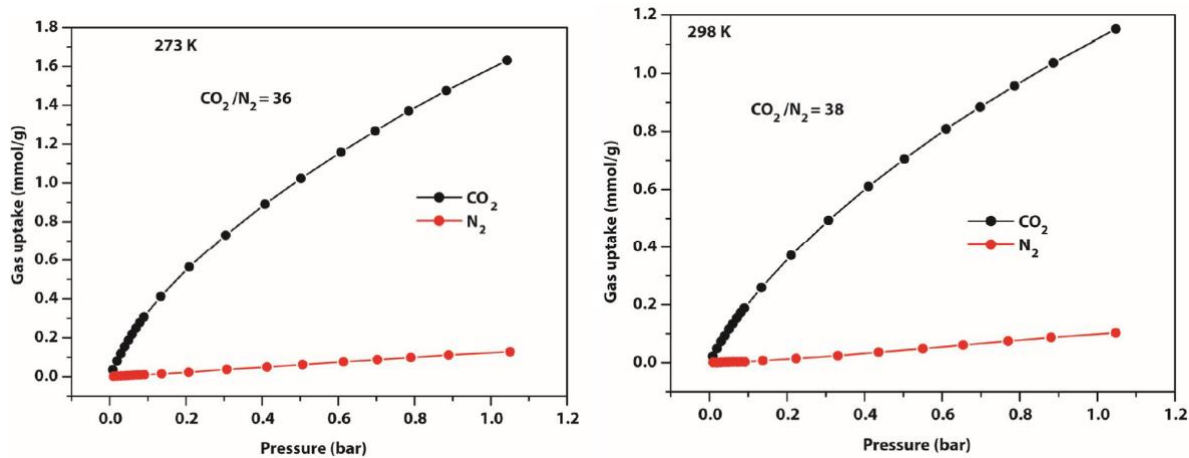


Figure S9. CO_2/N_2 selectivity of $\text{UiO}-66\text{-AB}$ at different temperatures estimated using the ratio of the initial slopes in the Henry regime of the adsorption.

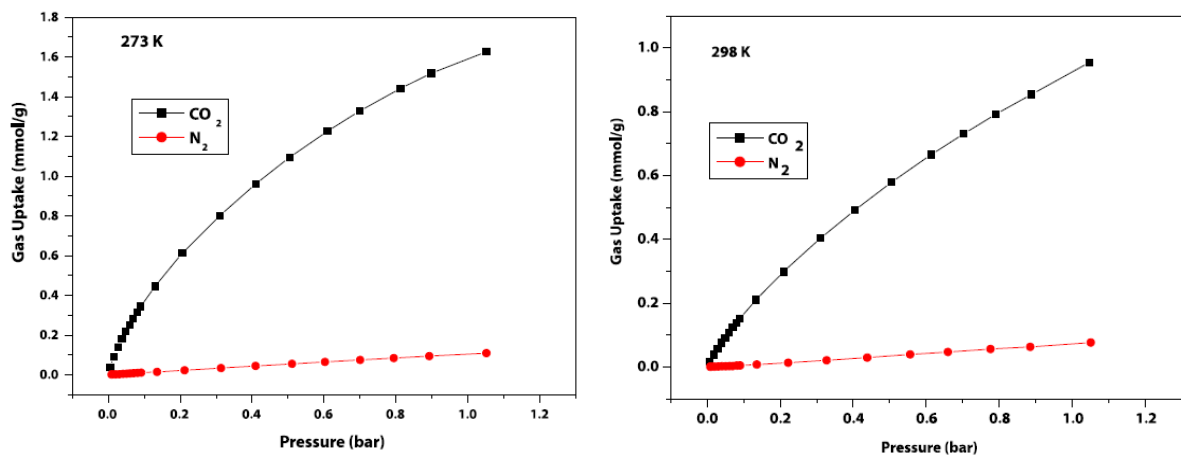


Figure S10. CO_2/N_2 selectivity of $\text{MIL-53}(\text{Al})\text{-AB}$ at different temperatures estimated using the ratio of the initial slopes in the Henry regime of the adsorption.

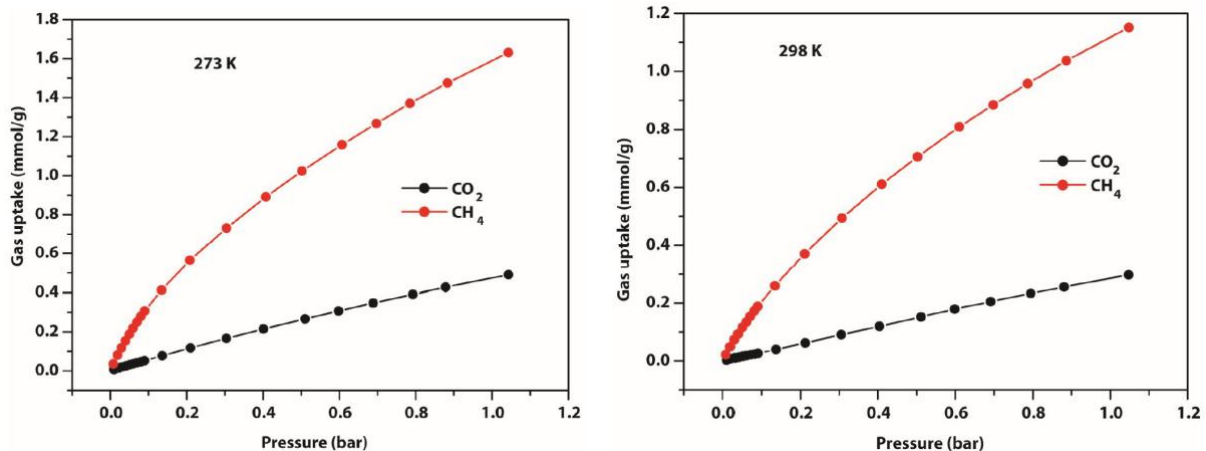


Figure S11. CO_2/CH_4 selectivity of $\text{UiO}-66\text{-AB}$ at two different temperatures estimated using the ratio of the initial slopes in the Henry regime of the adsorption.

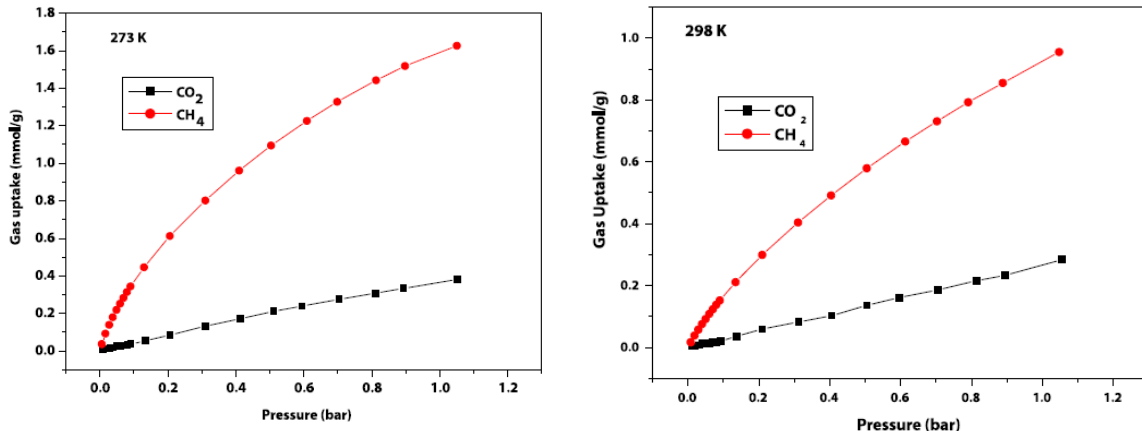


Figure S12. CO₂/CH₄ selectivity of MIL-53(Al)-AB wo different temperatures estimated using the ratio of the initial slopes in the Henry regime of the adsorption.

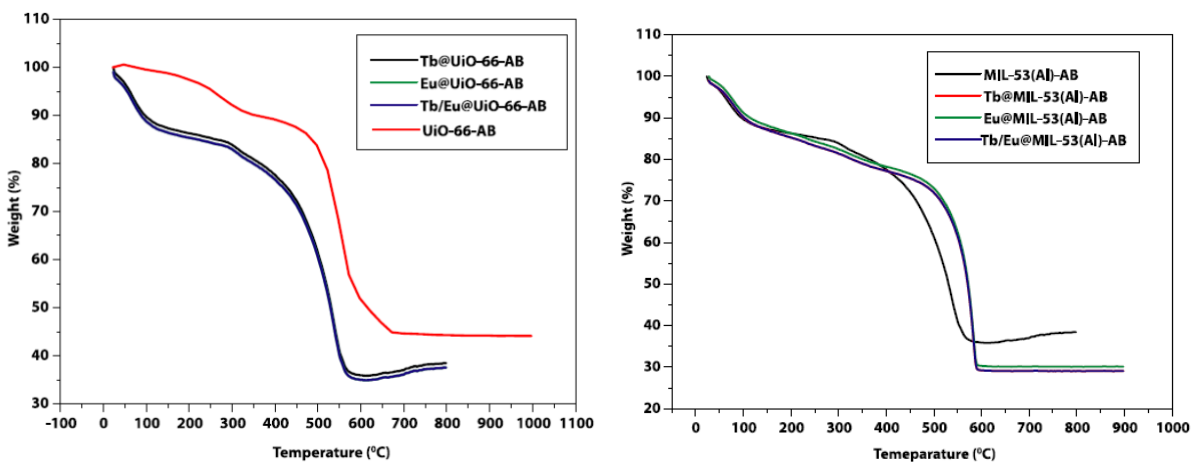


Figure S13. TGA analysis of Ln@UiO-66-AB (a) and Ln@MIL-53(Al)-AB (b).

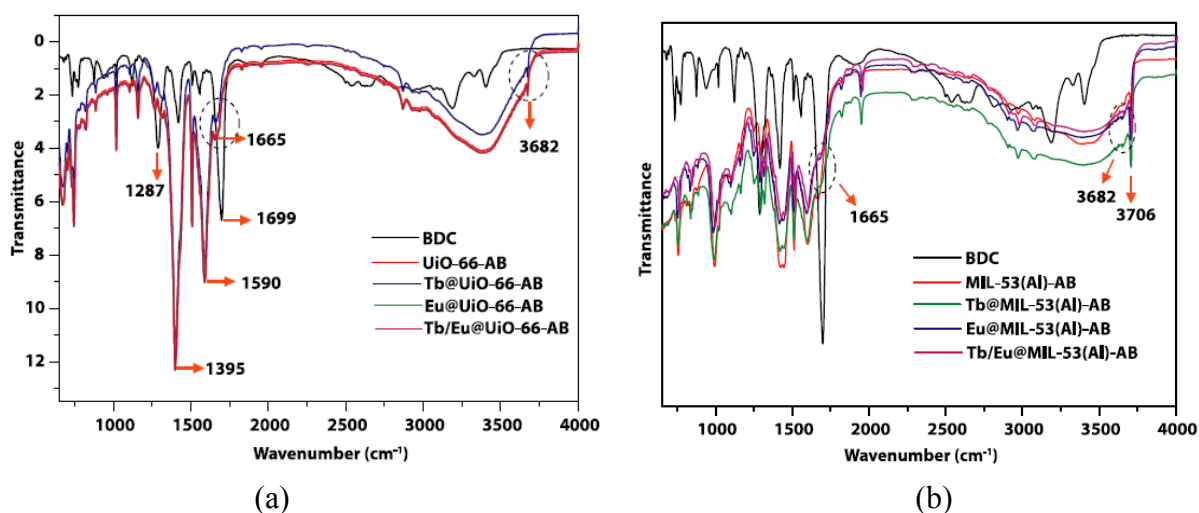


Figure S14. FT-IR analysis of Ln@UiO-66-AB (a) and Ln@MIL-53(Al)-AB (b) on comparison with terephthalic acid (BDC) and modulated MOFs.

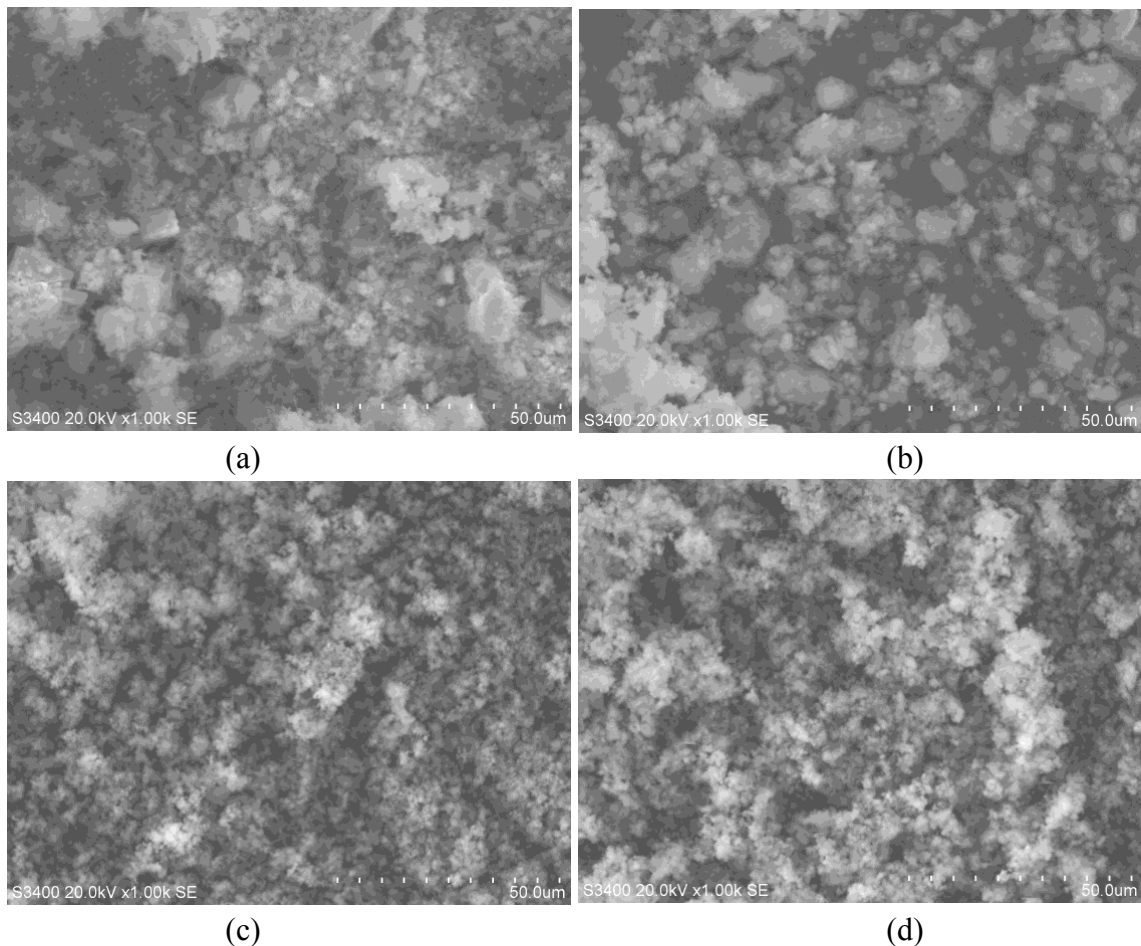


Figure S15. SEM micrographs of UiO-66-AB (a), Tb/Eu@UiO-66-AB (b), MIL-53(Al)-AB (c) and Tb/Eu@MIL-53(Al)-AB.

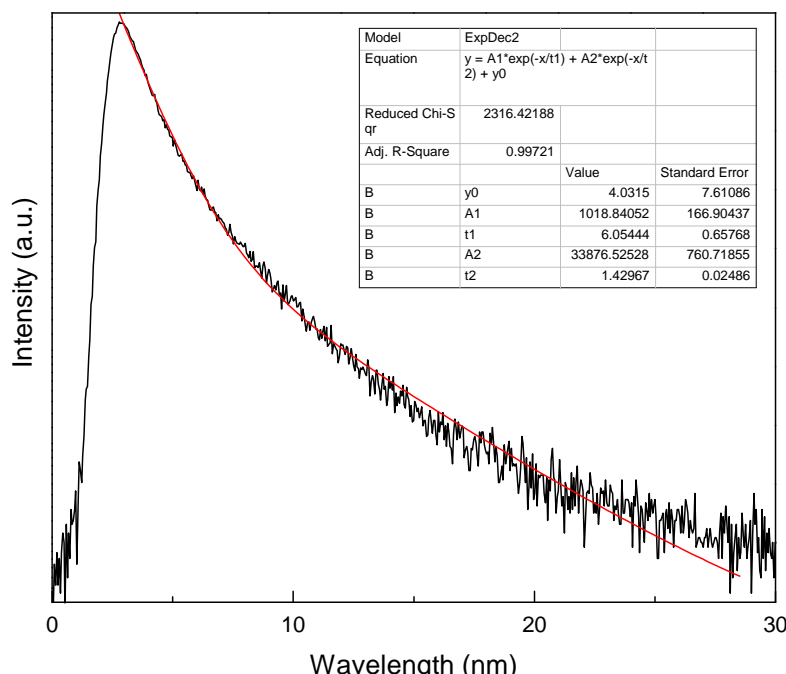


Figure S16. Luminescence decay profile of UiO-66-AB recorded when exciting at 410 nm and observing at 465 nm (excited at 410nm instead of 395nm due to equipment limitations).

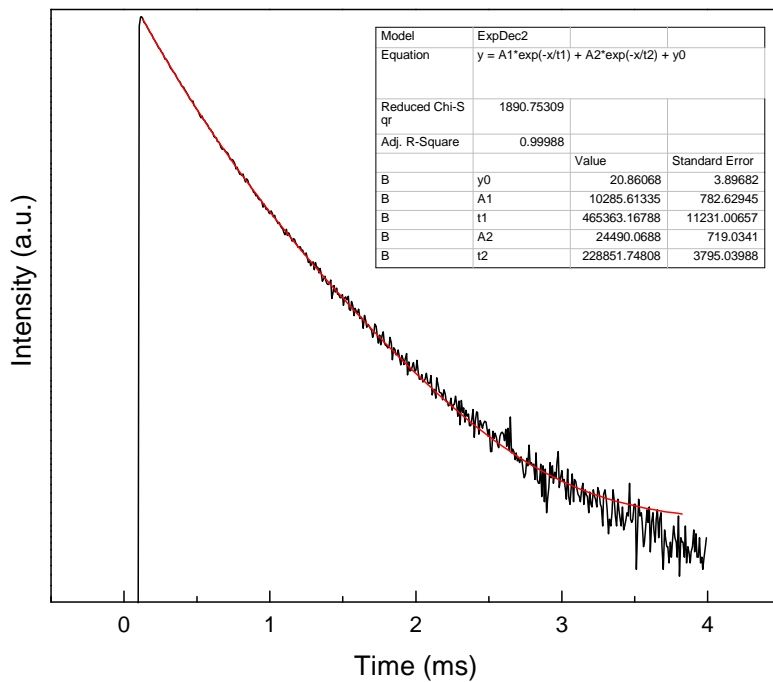


Figure S17. Luminescence decay profile of Eu@UiO-66-AB recorded when exciting at 307nm and observing at 612 nm.

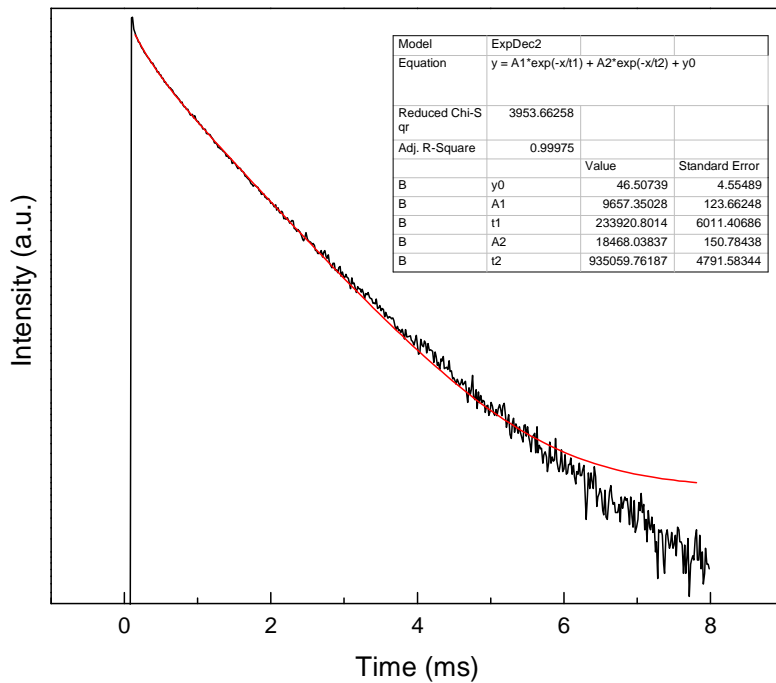


Figure S18. Luminescence decay profile of Tb@UiO-66-AB recorded when exciting at 307nm and observing at 542 nm.

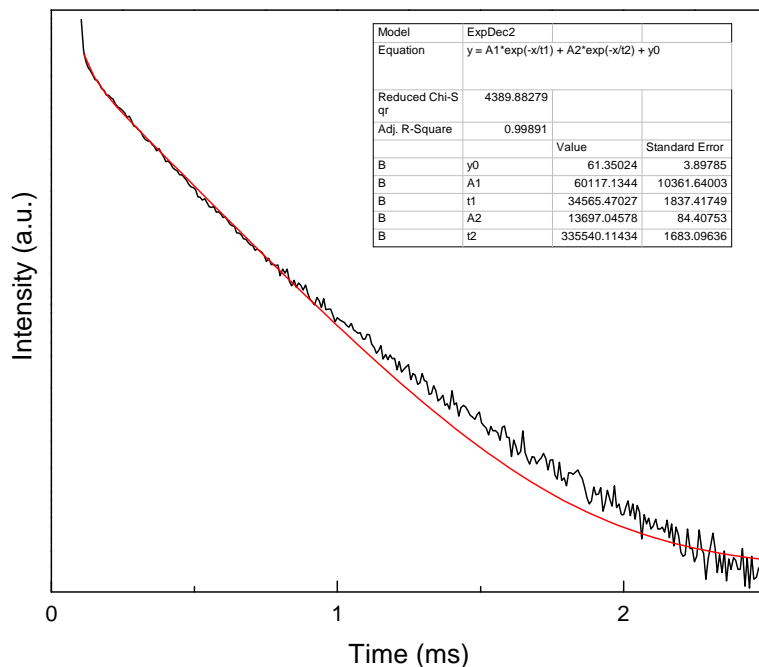


Figure S19. Luminescence decay profile of Tb/Eu@UiO-66-AB recorded when exciting at 300 nm and observing at 612 nm.

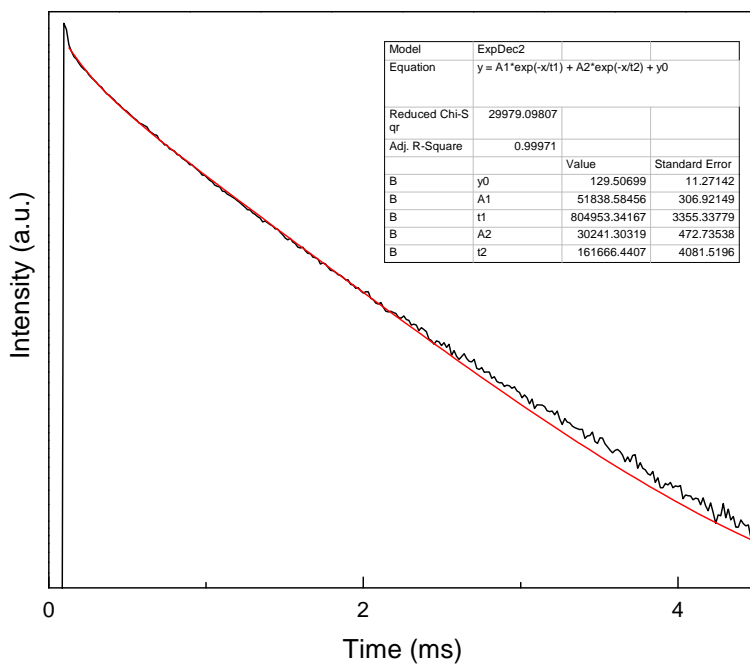


Figure S20. Luminescence decay profile of Tb/Eu@UiO-66-AB recorded when exciting at 300 nm and observing at 542 nm.

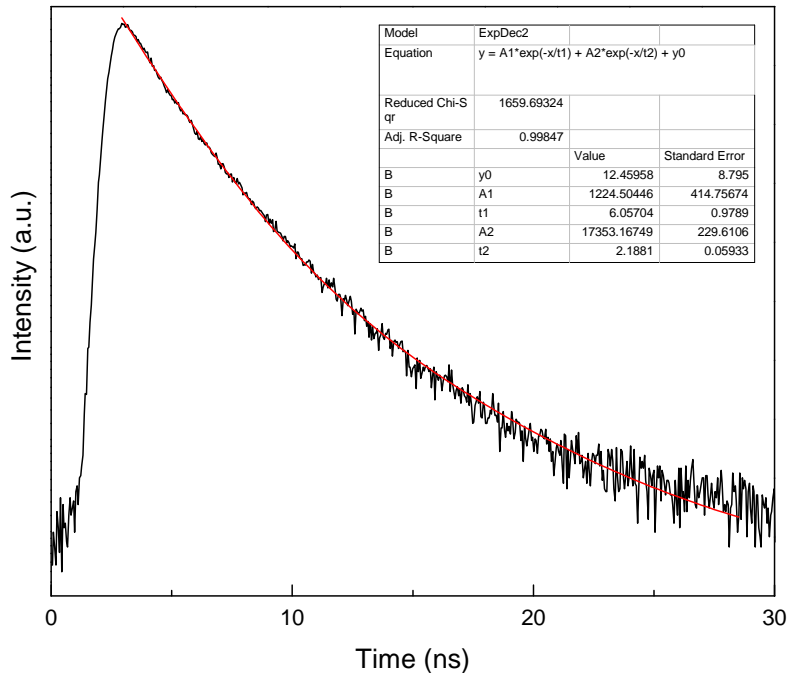


Figure S21. Luminescence decay profile of MIL-53(Al)-AB recorded when exciting at 410 nm and observing at 475 nm (excited at 410 nm instead of 394 nm due to equipment limitations).

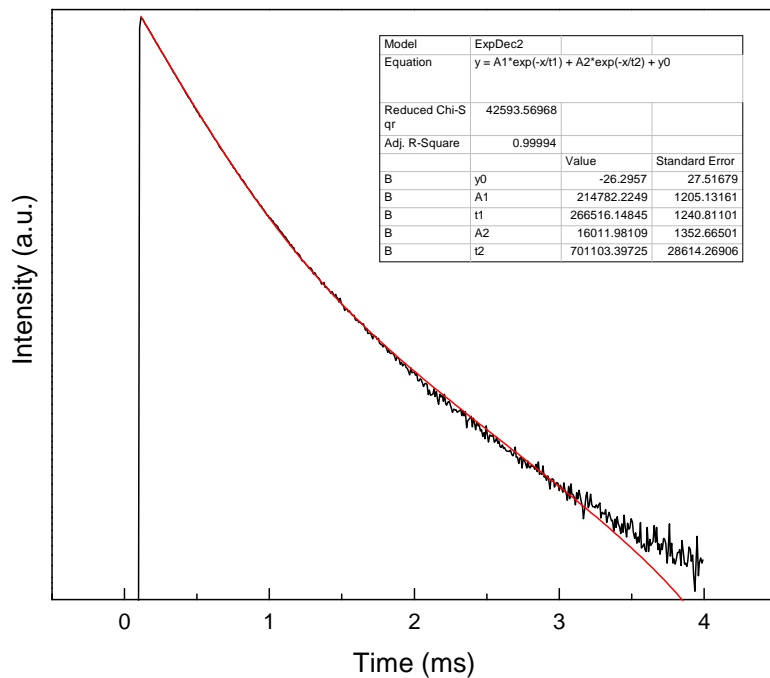


Figure S22. Luminescence decay profile of Eu@MIL-53(Al)-AB recorded when exciting at 302 nm and observing at 612 nm.

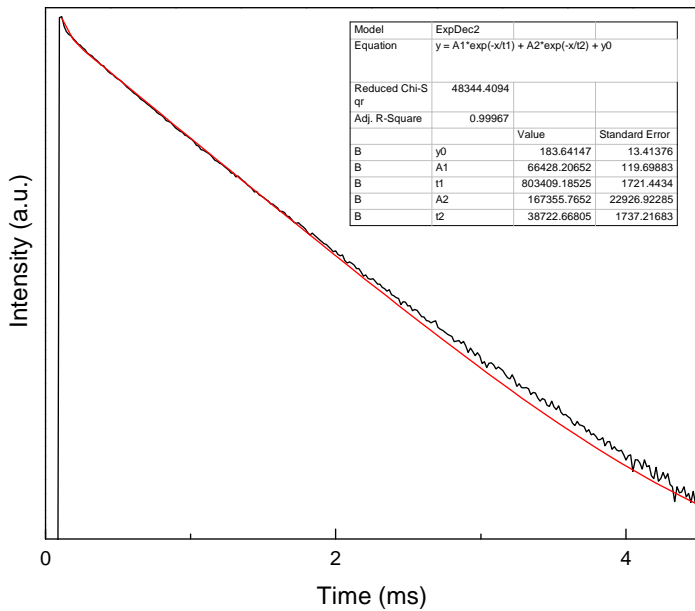


Figure S23. Luminescence decay profile of Tb@MIL-53(Al)-AB recorded when exciting at 302 nm and observing at 542 nm.

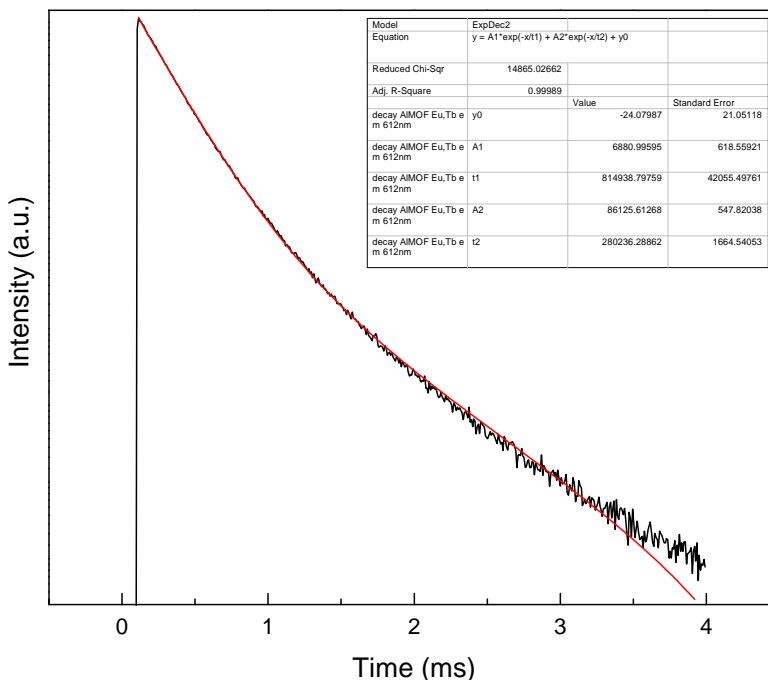


Figure S24. Luminescence decay profile of Tb/Eu@MIL-53(Al)-AB recorded when exciting at 300 nm and observing at 612 nm.

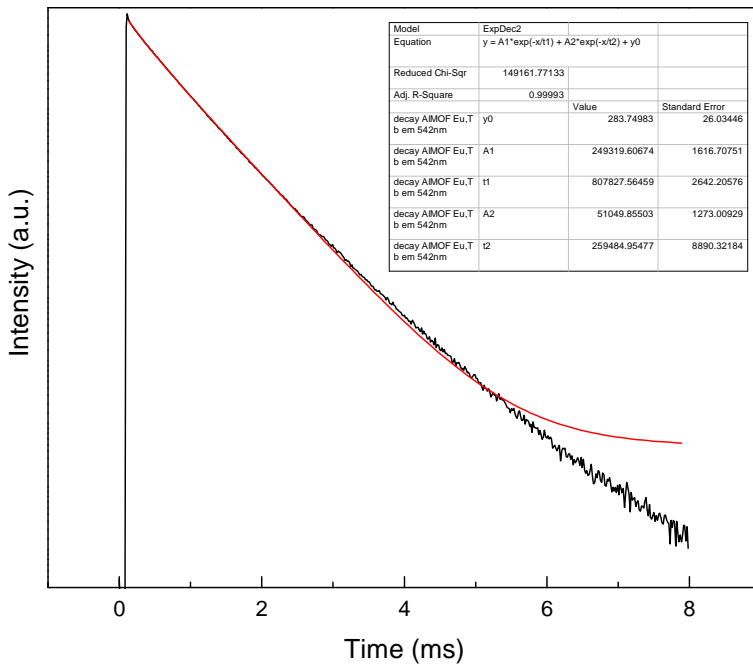


Figure S25. Luminescence decay profile of Tb/Eu@MIL-53(Al)-AB recorded when exciting at 300 nm and observing at 542 nm.

Discussion on the luminescence properties of lanthanide functionalized non modulated MOFs:

In order to compare the luminescent properties of Tb/Eu@UiO-66-AB and Tb/Eu@MIL-53(Al)-AB with lanthanide functionalized pristine (i.e. without the use of modulator) UiO-66 and MIL-53(Al), Tb/Eu@UiO-66 (pristine) and Tb/Eu@MIL-53(Al) (pristine) were synthesized in a similar way as lanthanide functionalized modulated MOFs. We observed lower surface area ($1194\text{ m}^2/\text{g}$) and reduced total pore volume ($0.791\text{ cm}^3/\text{g}$) of Tb/Eu@UiO-66 (pristine) in comparison to the non-doped UiO-66 ($1275\text{ m}^2/\text{g}$ and $0.80\text{ cm}^3/\text{g}$). Similar observation was noticed with lower surface area ($787\text{ m}^2/\text{g}$) and reduced total pore volume ($0.435\text{ cm}^3/\text{g}$) of Tb/Eu@MIL-53(Al) (pristine) in comparison to pristine MIL-53(Al) ($1224\text{ m}^2/\text{g}$ and $0.609\text{ cm}^3/\text{g}$). These observations confirm the lanthanide functionalization (Figure S26) in the respective pristine MOFs. Furthermore, the luminescent properties of Tb/Eu@UiO-66 (pristine) showed similar Tb^{3+} and Eu^{3+} luminescence properties as observed in Tb/Eu@UiO-66-AB (Figure S27). However, after several attempts with varying the excitation

wavelengths (280 – 340 nm), yellowish-white light was not observed for Tb/Eu@UiO-66 (pristine). Luminescent property of Tb/Eu@MIL-53(Al) was also carried out. This material showed similar Tb³⁺ and Eu³⁺ luminescence properties as observed in Tb/Eu@MIL-53(Al)-AB (Figure S28). However, after several attempts with varying the excitation wavelengths (280 – 340 nm), white light emission was not observed for Tb/Eu@MIL-53(Al).

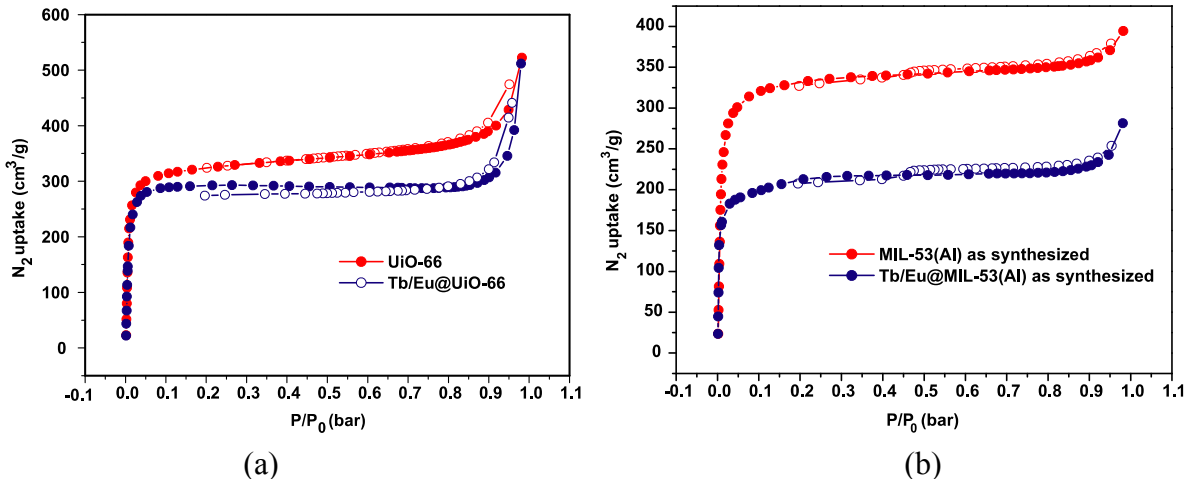
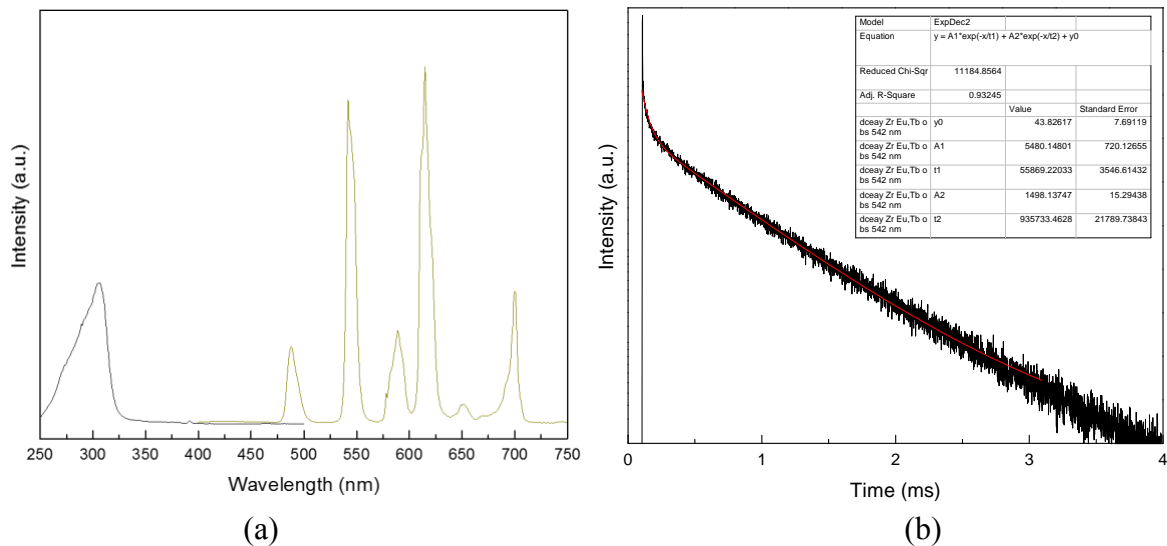
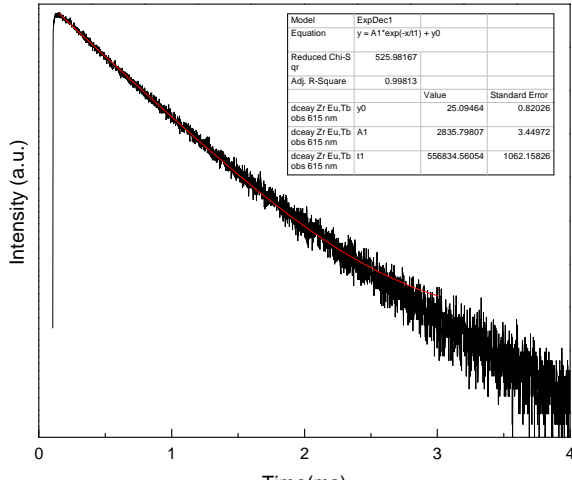


Figure S26. Comparison of nitrogen sorption isotherms of lanthanide functionalized pristine MOFs; Tb/Eu@UiO-66 (a) and Tb/Eu@MIL-53(Al) (b) with the respective pristine MOFs.





(c)

Figure S27. Combined RT excitation-emission spectra of Tb/Eu@UiO-66 excited at 300nm, observed at 542nm and 612 nm (a) and Luminescence decay profile recorded when exciting at 300 nm and observing at 542 nm (b) and 615 nm (c) respectively.

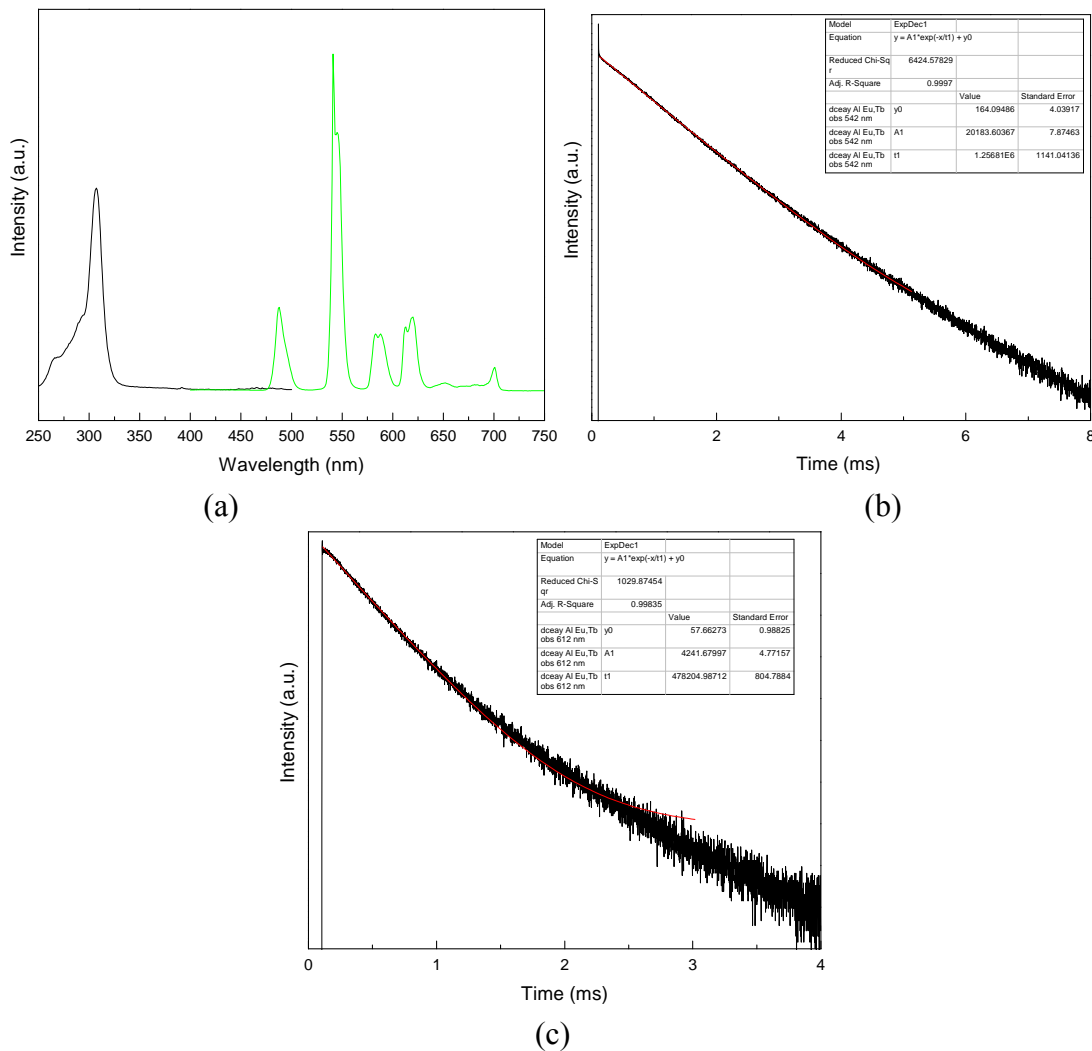


Figure S28. Combined RT excitation-emission spectra of Tb/Eu@MIL-53(Al) excited at 300nm, observed at 542nm and 612 nm (a) and Luminescence decay profile recorded when exciting at 300 nm and observing at 542 nm (b) and 612 nm (c) respectively.